Molecular and Cellular Neuroscience 94 (2019) 23–31

Contents lists available at ScienceDirect

Molecular and Cellular Neuroscience

journal homepage: www.elsevier.com/locate/ymcne

Cyclo(His-Pro) inhibits NLRP3 inflammasome cascade in ALS microglial cells

Silvia Grottelli[a], Letizia Mezzasoma[a], Paolo Scarpelli[a], Ivana Cacciatore[b], Barbara Cellini[a], Ilaria Bellezza[a,*]

[a] Department of Experimental Medicine, University of Perugia, Perugia, Italy
[b] Department of Pharmacy, "G. d'Annunzio" University of Chieti-Pescara, Chieti, Italy

ARTICLE INFO

Keywords:
NLRP3
Peroxynitrite
iNOS
NOX2
Caspase 1
SOD1 activity
Diketopiperazine

ABSTRACT

Neuroinflammation, i.e. self-propelling progressive cycle of microglial activation and neuron damage, as well as improper protein folding, are recognized as major culprits of neurodegenerative diseases, such as amyotrophic lateral sclerosis (ALS). Mutations in several proteins have been linked to ALS pathogenesis, including the G93A mutation in the superoxide dismutase 1 (SOD1) enzyme. SOD1(G93A) mutant is prone to aggregate thus inducing both oxidative stress and neuroinflammation. In this study we used hSOD1(G93A) microglial cells to investigate the effects of the antioxidant and anti-inflammatory cyclic dipeptide (His-Pro) on LPS-induced inflammasome activation. We found that cyclo(His-Pro) inhibits NLRP3 inflammasome activation by reducing protein nitration via reduction in NO and ROS levels, indicative of lower peroxynitrite generation by LPS. Low levels in peroxynitrite are related to NF-κB inhibition responsible for iNOS down-regulation and NO dampening. On the other hand, cyclo(His-Pro)-mediated ROS attenuation, not linked to Nrf2 activation in this cellular model, is ascribed to increased soluble SOD1 activity due to the up-regulation of Hsp70 and Hsp27 expression. Conclusively, our results, besides corroborating the anti-inflammatory properties of cyclo(His-Pro), highlight a novel role of the cyclic dipeptide as a proteostasis regulator, and therefore a good candidate for the treatment of ALS and other misfolding diseases.

1. Background

Amyotrophic lateral sclerosis (ALS) is a rare neurodegenerative disease linked to the progressive moto-neuron degeneration (Kiernan et al., 2011). About 90% of ALS cases are sporadic, but 5–10% of cases are inherited in an autosomal dominant fashion. Approximately 20% of familial are associated with mutations in the gene encoding superoxide dismutase 1 (SOD1) (Rosen et al., 1993) such as the substitution of glycine to alanine at position 93 (G93A). Mutant SOD1 exhibits a high aggregation tendency that renders the protein cytotoxic through a gain of function mechanism (Ruegsegger and Saxena, 2016). One of the possible cytotoxic mechanisms induced by protein aggregates is the ability to stimulate the inflammasome, a protein complex whose activation culminates in caspase 1 activation and mature IL-1β release (Shi et al., 2015). It is worth noticing that both active caspase 1 and IL-1β are elevated in the central nervous system of ALS mouse models and human subjects (Li et al., 2000; Meissner et al., 2010), pointing to a pivotal role of inflammasome in pathogenesis or progression of the disease (Volpe and Nogueira-Machado, 2015).

Generally, the activation of inflammasome depends on the binding of specific ligands, such as damage associated proteins (DAMPS) or pathogen specific proteins (PAMPS) to the inflammasome receptor, the most studied of which is NLRP3. The cytosolic ligand-receptor binding leads to the assembly of the inflammasome complex that culminates in caspase 1 recruitment and activation, which, in turn, is responsible for the cleavage/maturation of pro-IL-1β. Mature IL-1β is then released in

Abbreviations: ALS, amyotrophic lateral sclerosis; CHP, cyclo(His-Pro); COX2, cyclooxygenase2; DAMPS, damage associated proteins; DCFH-DA, 2′,7′-dichlorodihydrofluorescein diacetate; gp91phox, heme-binding membrane glycoprotein; Hsp, heat shock protein; iNOS, inducible nitric oxide synthase; IL-1β, interleukin 1beta; IL-6, interleukin 6; IL-17, interleukin 17; LC3, microtubule-associated protein 1 light chain 3; LPS, lipopolysaccharide; NF-κB, nuclear factor kappa-B; NLRP3, NLR family, pyrin domain containing 3; NO, nitric oxide; NOX2, NADPH oxidase 2; Nrf2, NF-E2-related factor 2; PAMPS, pathogen specific proteins; p47phox, NADPH oxidase subunit (47 kDa); ROS, reactive oxygen species; SOD1, superoxide dismutase 1; ThT, thioflavin T; TLR4, toll-like receptor 4; TNFα, tumor necrosis factor alpha

* Corresponding author at: Department of Experimental Medicine, p.le Severi, University of Perugia, 06132 Perugia, Italy.
E-mail address: ilaria.bellezza@unipg.it (I. Bellezza).

https://doi.org/10.1016/j.mcn.2018.11.002
Received 2 August 2018; Received in revised form 31 October 2018; Accepted 11 November 2018
Available online 13 November 2018
1044-7431/

the extracellular milieu to elicit its effects in an autocrine/paracrine manner. It is worth noticing that IL-1β secretion requires a two-step mechanism: (i) a priming step, i.e. NF-κB-driven pro-IL-1β gene expression, and (ii) a maturation step, i.e. the caspase-1 dependent pro-IL-1β cleavage. IL-1β promotes several pro-inflammatory reactions and has been closely associated to neuroinflammation and the associated brain diseases (Singhal et al., 2014).

The primary mediators of neuroinflammation are microglial cells that represent the innate immune mononuclear phagocytes of the central nervous system. We recently showed that murine microglial cells harbouring the G93A mutation in the SOD1 gene respond to inflammatory stimuli by activating NLRP3 inflammasome (Bellezza et al., 2018). Neuroinflammatory reactions lead to the activation and nuclear translocation of the transcription factor NF-κB that, in turn, positively controls the expression of both pro-inflammatory cytokines, e.g. IL-6, IL-1β and TNFα, and of pro-inflammatory enzymes, such as COX2 and iNOS, the latter responsible for an increase in nitric oxide (NO) levels. Moreover, in the course of an inflammatory response, microglial cells increase the expression and activity of the enzyme NADPH oxidase 2 (NOX2), responsible for the production of superoxide anion, thus causing an increase in ROS levels, an event known as oxidative stress. The simultaneous increase in NO and ROS levels is known as nitro-oxidative stress. We have demonstrated that inflammasome activation, in the ALS microglial cell model, depends on the induction of nitro-oxidative stress and that the inhibition of the activity of iNOS and NOX2 abolish caspase 1 activity (Bellezza et al., 2018).

Cyclo(His-Pro), an endogenous cyclic dipeptide derived from the cleavage of thyreotropin releasing hormone, elicits both anti-inflammatory and anti-oxidative effects in several cellular and animal models of neurodegeneration (Grottelli et al., 2016). Cyclo(His-Pro) suppress LPS-induced activation of NF-κB in BV2 microglial cells, thus leading to the reduction of cytokine production and iNOS and COX2 expression. These effects render cyclo(His-Pro) a potential anti-inflammatory molecule. On the other hand, the antioxidant properties of cyclo(His-Pro) rely on its ability to reduce ROS generation through the activation of the transcription factor Nrf2, which results in the increased expression of a plethora of antioxidant genes (Grottelli et al., 2016; Bellezza et al., 2014a).

Due to the ability of cyclo(His-Pro) to counteract both oxidative and nitrosative stress, we aimed at testing whether the cyclic dipeptide can dampen inflammasome activation in the hSOD1(G93A) microglial cells, used as cellular model of ALS.

2. Materials and methods

2.1. Materials

Cyclo(His-Pro) (CHP) was synthesized as described elsewhere (Kukla et al., 1985). All the reagents, unless otherwise stated, were from Sigma-Aldrich (St. Louis, MO). All the antibodies, unless otherwise stated, were from Santa Cruz Biotech (Santa Cruz, CA). Cell culture reagents were from Life Technologies (GibcoBRL, Gaithersburg, MD).

2.2. Immortalized microglia

Immortalized microglial cells, obtained from embryonic (E14) cortices from hSOD1(G93A) mice following the method described by Righi et al. (1989), were a kind gift of Dr G. Pietrini (Università di Milano). Microglia were characterized by Western blot and immunofluorescence for the presence of selective markers (CSF-1) and the absence of astrocyte-specific molecules (i.e., glial fibrillary acidic protein).

2.3. Cell cultures and treatments

hSOD1(G93A) microglial cells were cultured in DMEM F-12 supplemented with 5% foetal bovine serum (FBS), glutamine (4 mM), penicillin (50 U/ml), and streptomycin (50 mg/ml) at 37 °C in a humidified 5% CO_2 environment and seeded at the density of 31,000/cm^2. After 24 h subculture, cells were treated with 50 μM CHP and then exposed to 1 μg/ml LPS for various time. In Thioflavin T experiments cell were grown for four days in the presence of 50 μM CHP.

Human THP-1 monocytes were purchased from American Type Culture Collection (ATCC, USA) and routinely maintained at 37 °C in 5% CO_2 in RPMI 1640 supplemented with 10% FBS, glutamine (4 mM), penicillin (50 U/ml), and streptomycin (50 mg/ml) at 37 °C in a humidified 5% CO_2 environment and seeded at the density of (1×10^6 cells/ml). After 24 h subculture, cells were treated with 50 μM CHP and then exposed 10 μg/ml LPS/5 mM ATP for 60 min.

2.4. Measurement of NO production

Nitric oxide (NO) production was determined indirectly through the measurement of nitrite, a stable metabolite of nitric oxide, by Griess reaction. After the treatments, a 50 μl aliquot of culture medium was mixed with an equal volume of Griess reagent, incubated for 20 min at room temperature and absorbance read at 550 nm using a microplate reader (Seac, Florence, Italy). Results were expressed as percentage of the control, assumed as 100%. Nitrite standard reference curve was prepared for each determination.

2.5. Measurement of cytokine levels by ELISA

Cytokine production was measured with an enzyme-linked immunosorbent assay (ELISA) kit in cell medium collected from control/LPS-treated cells. Samples were analysed according to the manufacturer's protocols (BD Biosciences Pharmingen, San Diego, CA).

2.6. Real time PCR

Total RNA was isolated with TRIZOL Reagent (Invitrogen Ltd., Paisley, UK) according to the manufacturer's instructions and cDNA was synthesized using iScript cDNA synthesis kit (Bio-Rad Lab, Hercules, CA.). Real time PCR was performed using the iCycler iQ detection system (Bio-Rad) and SYBR Green chemistry. Mouse primer sequences, obtained from Invitrogen (Invitrogen Ltd., Paisley, UK) were listed in Table 1. SYBR Green RT-PCR amplifications were carried out in a 96-well plate in a 25 μl reaction volume that contained 12,5 μl of 2× iQ™ SYBR® Green SuperMix (Bio-Rad), 400 nM forward and reverse primers, and 5 to 40 ng of cDNA. In each assay, no-template controls were included and each sample was run in triplicates. The thermal profile consisted of incubation at 95 °C 3 min, followed by 40 cycles of denaturation for 10 s at 95 °C and an annealing/extension step of 30 s at 62 °C. Mean of Ct values of the stimulated sample was compared to the untreated control sample. ΔCt is the difference in Ct values derived from the target gene (in each assayed sample) and Gapdh, while ΔΔCt represents the difference between the paired samples. The n-fold differential ratio was expressed as $2^{-\Delta\Delta Ct}$.

2.7. Western blotting analyses

Cells were lysed in boiling Laemmli sample buffer or processed with NE-PER(R) Nuclear and Cytoplasmic Extraction Reagents (Pierce Biotechnology, Rockford, IL) according to manufacturer's instruction. Extracts were loaded on SDS-polyacrylamide gel, transferred on nitrocellulose membrane and immunoblotted with Phospho-NF-kB p65 (Ser536) antibody (1:1000) (#3036), caspase 1 antibody (1:1000) (#2225; Cell Signalling Technology, Danvers, MA), iNOS (M-19) antibody (1:200), Nrf2 (C-20) antibody (1:200), LC3 antibody (1:1000) (#L-8918; Sigma-Aldrich, St. Louis, MO), Ubiquitinylated proteins (FK2) antibody (1:2000) (Merck Millipore, Darmstadt, Germany) and horseradish peroxidase-conjugated-anti IgG antibody (1:5000). GAPDH (6-C5) antibody (1:5000), Lamin B (C-20) antibody (1:100), and β-actin

Table 1
List of primers.

Gene name	Gene symbol	Primer sequences (F. forward; R. reverse)
Glyceraldehyde-3-phosphate-dehydrogenase	Gapdh	F. GCCAAATTCAACGGCACAGT R. AGATGGTGATGGGCTTCCC
Interleukin 1beta	IL1β	F. AAAAGCCTCGTGCTGTCGGACC R. TTGAGGCCCAAGGCCACAGGT
Interleukin 6	IL6	F. GCTGGAGTCACAGAAGGAGTGGC R. GGCATAACGCACTAGGTTTGCCG
Tumor necrosis factor alpha	Tnfα	F. GCCCACGTCGTAGCAAACCAC R. GGCTGGCACCACTAGTTGGTTGT
NLR family, pyrin domain containing 1A	Nlrp1a	F. CTTGAGAAGTTGGGTGGGGT R. GATGGAGCAACTCAGGACCA
NLR family, pyrin domain containing 3	NLRP3	F. GACACGAGTCCTGGTGACTTT R. CAGACGTATCTGAGCCAT
NLR family, CARD domain containing 4	IPAF	F. TCAGGTCACAGAAGACCT R. TTCACCCAGGGGGTAGAAGT
Absent in melanoma 2	Aim2	F. AAAACTGCTCTGCTGCCTCT R. GATGGCTTCCTGTTCTGCCA
PYD and CARD domain containing	Asc	F. AACTGCGAGAAGGCTATGGG R. TGAGCTCCAAGCCATACGAC
Heme-binding membrane glycoprotein gp91phox	gp91phox	F. TCACCACTAGTACCAGCATCACCA R. ACTCTGTCTTGCATTTCTGGATGCC
NADPH oxidase subunit (47 kDa)	p47phox	F. GGTCGACCATCCGCAACGCA R. TGTGCCATCCGTGCTCAGCG
Inducible Nitric Oxide synthase	iNOS	F. GGTGTTCTTTGCTTCCATGCTAAT R. GTCCCTGGCTAGTGCTTCAGA
Glutamate cysteine ligase catalytic subunit	Gclc	F. GGCGATGTTCTTGAGACTCTGC R. TTCCTTCGATCATGTAACTCCC
Glutamate cysteine ligase modifier subunit	Gclm	F. CACAGGTAAAACCCAATAGTAACCAAGT R. GTGAGTCAGTAGCTGTATGTCAAATTGTT
Peroxiredoxin 1	Prdx1	F. TTGGCGCTTCTGTGGATTCT R. GGTGCGCTTGGGATCTGATA
NAD (P)H: quinone oxidoreductase 1	Nqo1	F. GGCTGGTTTGAGAGAGTGCT R. TCTGGAAAGGACCGTTGTCG
Glutathione peroxidase	Gpx	F. CAGTTCGGAACATCAGGAAGAAT R. AGAGCGGGTGAGCCTTCT
Heat shock protein 27	Hsp27	F. CACTGGCAAGCACGAAGAAAG R. GCGTGTATTTCCGGGTGAAG
Heat shock protein 70	Hsp70	F. AGCTGGACAAGTCACAGATC R. GGTGTCTCCAGCTGTTGATT
Heat shock protein 72	Hsp72	F. TTTGTCCTGCAATCAAGTCCT R. GGCTGTCCTGCAAAACAAAT

(I-19) antibody (1:400) were used as marker proteins for total and nuclear extracts. Immunocomplexes were visualized with an enhanced chemiluminescence kit (ECL, Pierce Biotechnology, Rockford, IL). Band intensity was analysed by InageJ software.

2.8. Measurement of intracellular fluorescence

hSOD1(G93A) microglial cells, seeded on glass coverslips, were used for the following evaluations:

2.8.1. ROS production

The 2′,7′-dichlorodihydrofluorescein diacetate (DCFH-DA) method was used to detect ROS intracellular levels (Eruslanov and Kusmartsev, 2010). Cells were loaded with DCFH-DA (10 μM) for 30 min at 37 °C, and fixed with PFA 4% for 20 min at room temperature. The fluorescence of 2′,7′-dichlorofluorescein was detected at 485 nm excitation and at 535 nm emission.

2.8.2. Detection of activate caspase 1

hSOD1(G93A) cells were loaded with 50 μM caspase 1 fluorogenic peptide substrate (Ac-YVAD-AFC) for 1 h at 37 °C, and fixed for 20 min in 4% PFA at room temperature.

2.8.3. Immunolocalization of nitrated protein

Cells were fixed with PFA 4% for 20 min at room temperature and incubated overnight at 4 °C with nitrotyrosine antibody (1:50) (Sigma-Aldrich, St. Luis, MO). Cells were then incubated with Cyanine Cy™ 3 anti-rabbit IgG (1:100) (Jackson ImmunoResearch Laboratories, Inc., PA, USA) for 1 h at room temperature. Control samples were incubated with non-immune serum.

2.8.4. Actin labelling

Phalloidin was used to detect filamentous actin (F-actin) content on hSOD1(G93A). The cells were fixed with 4% PFA for 20 min at room temperature and F-actin was stained with tetramethylrhodamine (TRITC)-labelled phalloidin (1:250) for 30 min at room temperature.

At the end of each experimental procedure, cell nuclei were counterstained with 4′, 6-diamidino-2phenylindole (DAPI) and samples were analysed with a Zeiss Axio Observer Z1 equipped with Apotome and digital Camera Axiocam MRm (Zeiss).

2.9. SOD1 specific activity

Cell pellets from hSOD1(G93A) cells were treated with CHAPS buffer (1% w/v CHAPS, 100 mM KCl, 20 mM Hepes, 1 mM EGTA), pH 8 plus protease inhibitor cocktail (CompleteMini, Roche) for 30 min at 4 °C. The whole cell extract was separated by centrifugation (12,500 × *g*, 10 min, 4 °C) to obtain the soluble fraction. The pellets were then re-suspended in an equal volume of CHAPS buffer to obtain the insoluble fraction. Protein extract was incubated with a SOD1 reaction mixture (50 mM potassium phosphate pH 7.8, 0.1 mM EDTA, 0.01 mM cytochrome *c*, 0.05 mM xanthine, 0.005 unit of xanthine

oxidase) at 25 °C and spectrophotometrically monitored. One unit of SOD was defined as the amount of enzyme required to cause 50% inhibition of cytochrome *c* reduction traced at 550 nm and expressed as Units/mg protein.

2.10. Thioflavin T fluorescence

The Thioflavin T (ThT) assay was used to measure changes of fluorescence intensity of ThT upon binding to protein aggregates. Briefly, cells were seeded in 6-well plate for four days in the presence or in the absence of 50 μM CHP. Proteins extract (50 μg) from control and CHP treated cells were loaded with 50 μM ThT for 1 h at 37 °C. The fluorescence of ThT was detected at 440 nm excitation and at 490 nm emission with Infinite M200 (Tecan).

2.11. Statistical analysis

All the results were confirmed in at least three separate experiments performed as a minimum in quadruplicate. Data were analysed for statistical significance by Mann-Whitney *U* test. *p*-Values < 0.05 were considered significant and indicated as *.

3. Results

3.1. Cyclo(His-Pro) inhibits NLRP3 inflammasome in hSOD1(G93A) microglial cells

We have previously shown that LPS can activate NLRP3 inflammasome in hSOD1(G93A) microglial cells via induction of nitro-oxidative stress (Bellezza et al., 2018). Based on the known anti-inflammatory (Bellezza et al., 2014b) and anti-oxidative properties of

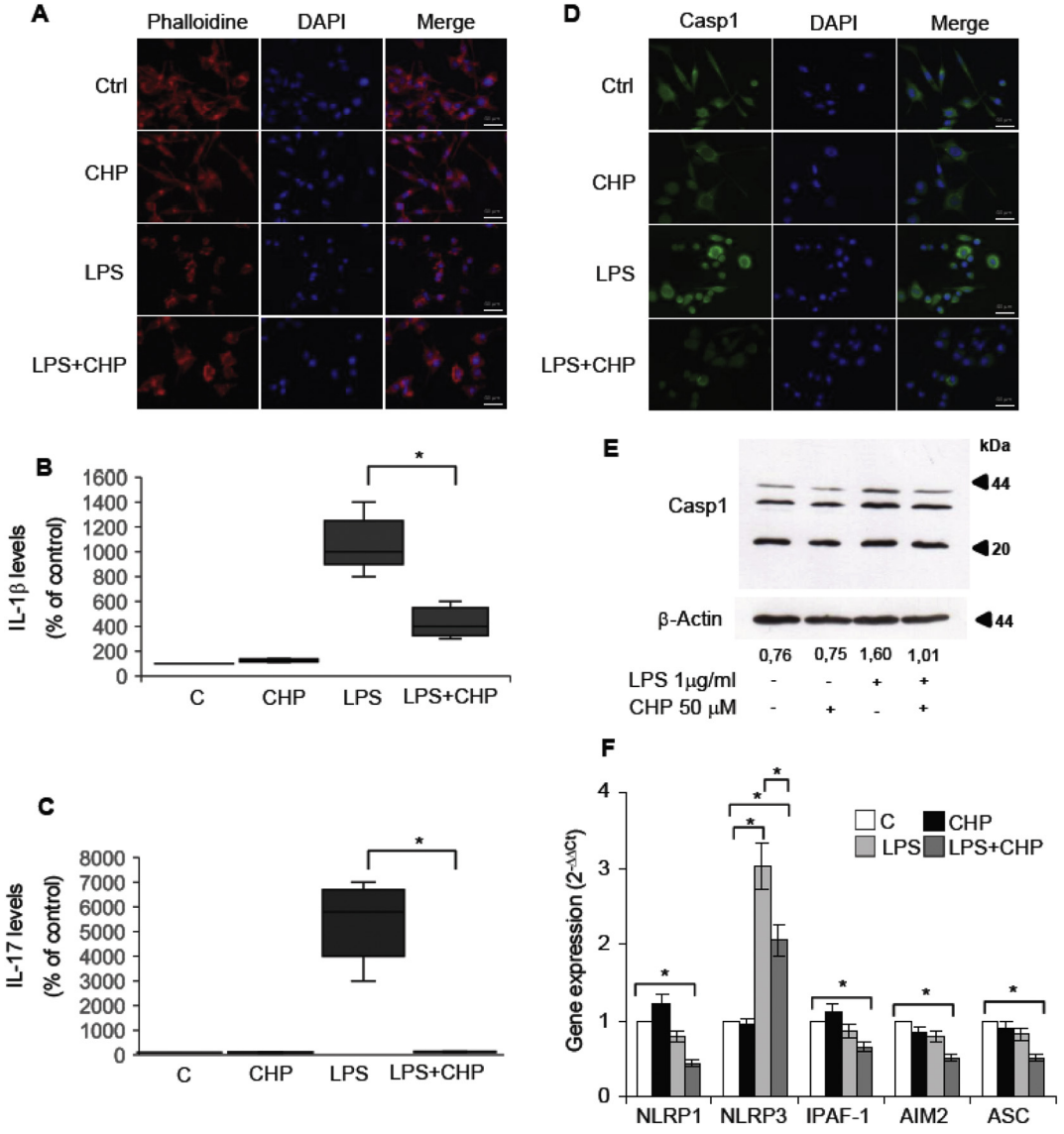

Fig. 1. Cyclo(His-Pro) inhibits NLRP3 inflammasome. hSOD1(G93A) microglial cells were pretreated for 24 h with 50 μM CHP and then exposed to 1 μg/ml LPS. (A) Phalloidin staining after 24 h LPS exposure. Magnification 40×. The images are representative of one out of three separate experiments; (B) IL-1β and (C) IL-17 secretions assayed in cell medium by ELISA after an 18 h LPS treatment. Concentration of cytokines secreted by control cells (IL-1β 15 ± 0.98 pg/ml; IL-17 50 ± 4.6 pg/ml) was assumed as 100%. Data represent mean ± SD ($n = 3$). *$p < 0.05$; (D) detection of activated caspase 1 by immunofluorescence, magnification 40×; and (E) Western Blotting analysis of full length and cleaved caspase 1 after a 6 h LPS exposure. β-actin was used as loading control and numbers below the images represent the ratio between p20 fragment and β-actin band intensity. The images are representative of one out of at least three separate experiments; (F) qRT-PCR of the indicated genes after a 3 h LPS exposure. Gene expression values were normalized to Gapdh and presented as $2^{-\Delta\Delta Ct}$. Relative mRNA gene abundance in untreated cells was assumed to be 1 (control). Data represent mean ± SD ($n = 3$). *$p < 0.05$.

cyclo(His-Pro) (Minelli et al., 2009a, 2009b; Grottelli et al., 2015), we sought to determine whether the cyclic dipeptide could affect inflammasome activation in the same cellular model. We first evaluated the ability of cyclo(His-Pro) to revert the morphological changes characteristic of microglial activation induced by LPS. In the presence of 50 μM cyclo(His-Pro), hSOD1(G93A) microglial cells display a morphology similar to control cells, suggesting that the cyclic dipeptide can reduce microglial activation. Indeed, in the presence of 1 μg/ml LPS microglial cells assume an amoeboid phenotype characteristic of activated microglia (Fig. 1A). Being inflammasome one of the key players in microglial activation, we analysed the effect of cyclo(His-Pro) on inflammasome activation (Fig. 1B, C and D). The pre-treatment of hSOD1(G93A) microglial cells with 50 μM cyclo(His-Pro) significantly reduces LPS-induced secretion of IL-1β (Fig. 1B) and IL-17 (Fig. 1C). Moreover, cyclo(His-Pro) dampens active caspase 1, as shown by a reduction in the cleavage of the fluorescent diffusible substrate YVAD (Fig. 1D) and a reduction in the amount of the cleaved p20 fragment (Fig. 1E). Similar results have been obtained in human THP-1 cells exposed to cyclo(His-Pro) before LPS plus ATP treatment (Supplementary Fig. 1). To determine the involvement of NLRP3 inflammasome receptor in cyclo(His-Pro) induced effects, we analysed gene expression of inflammasome related genes (Fig. 1F). Cyclo(His-Pro) significantly reduces NLRP3 gene expression which undergoes a three-fold increase in the presence of LPS. It is of interest that treatment with cyclo(His-pro) prior to the LPS exposure significantly reduces the expression of all the examined inflammasome components (Fig. 1E). These data indicate that the cyclic dipeptide can reduce neuroinflammation by inhibiting inflammasome activation.

3.2. Cyclo(His-Pro) reduces protein nitration in hSOD1(G93A) microglial cells

We have previously shown that LPS-induced inflammasome activation depends on peroxynitrite formation (Bellezza et al., 2018). To understand whether cyclo(His-Pro)-induced inhibition of inflammasome depends on the reduction of peroxynitrite production, we analysed nitrotyrosine levels in hSOD1(G93A) microglial cells (Fig. 2A) and found a reduced nitrotyrosine immunoreactivity in the presence of the cyclic dipeptide. Peroxynitrite, responsible for protein nitration, is produced by the spontaneous reaction of superoxide anion with NO (Ferrer-Sueta and Radi, 2009). To investigate the mechanism by which cyclo(His-Pro) induces a decrease in protein nitration, we determined both ROS and NO levels after LPS exposure (Fig. 2B and C) and found that both were reduced by pre-treatment with cyclo(His-Pro). It is to note that LPS caused a small but significant decrease in cell viability, an effect that was completely reversed by cyclo(His-Pro) (Fig. 2C). These data suggest that cyclo(His-Pro) can inhibit inflammasome activation by reducing peroxynitrite formation.

3.3. Cyclo(His-Pro) reduces NO production by inhibiting NF-κB in hSOD1(G93A) microglial cells

It is well recognized that LPS, by inducing the activation of the transcription factor NF-κB, can increase the production of both ROS and NO by up-regulating NOX2 and iNOS expression, respectively (Doyle and O'Neill, 2006). To test whether cyclo(His-Pro)-induced reduction in protein nitration depends on NF-κB inhibition, we analysed the phosphorylation levels of NF-κB p65 subunit and found that cyclo(His Pro) strongly reduces p65 phosphorylation induced by a 3 h exposure to LPS (Fig. 3A). To determine whether p65 phosphorylation correlates with NF-κB activation, we measured the mRNA levels of several NF-κB driven genes. We found that cyclo(His-Pro) significantly decreases LPS-induced IL-6 and iNOS mRNA levels whereas the cyclic dipeptide does not modify the expression of the other analysed genes (Fig. 3B–F). The reduced iNOS gene expression correlates with its protein expression (Fig. 3G), as detected by Western blotting, and can explain the reduced

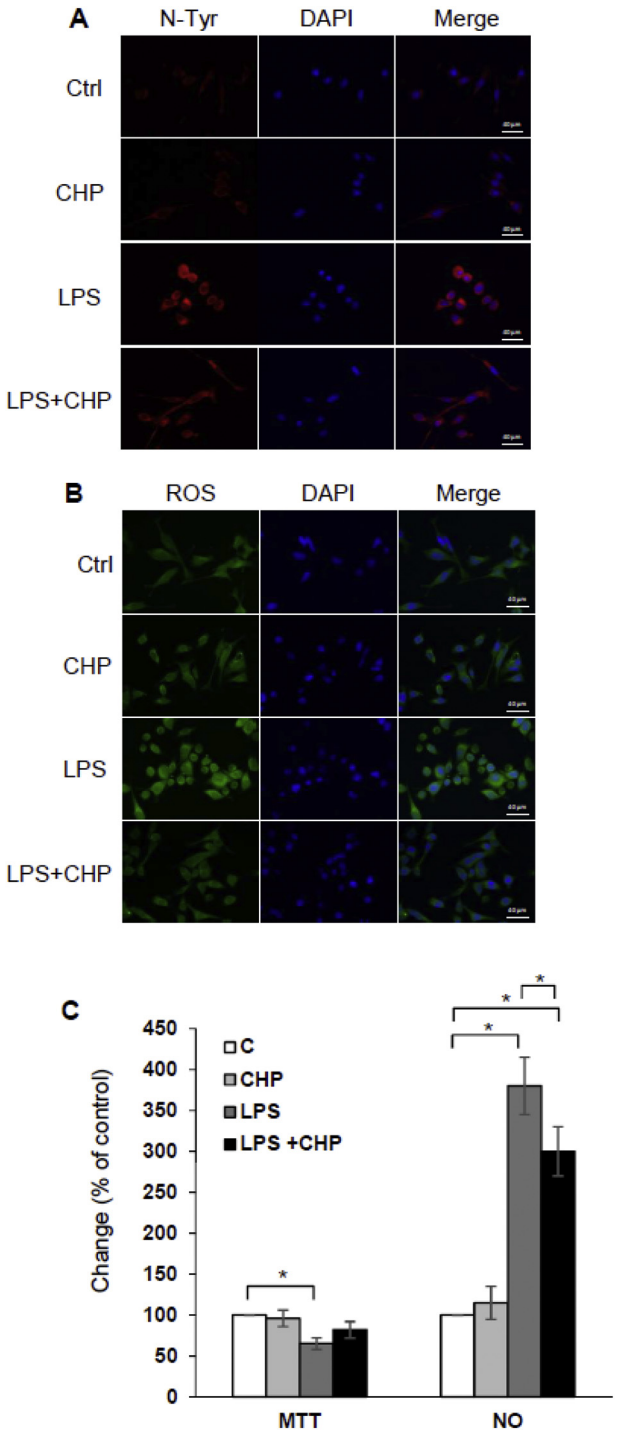

Fig. 2. Cyclo(His-Pro) reduces protein nitration. hSOD1(G93A) microglial cells, pretreated with 50 μM CHP for 24 h, were exposed to 1 μg/ml LPS and used for (A) immunolocalization of nitrotyrosine using anti-nitrotyrosine antibody after a 6 h LPS exposure. Magnification 40×. The images are representative of one out of three separate experiments; (B) detection of ROS generation by DCF fluorescence after a 24 h LPS exposure. Magnification 40×. The images are representative of one out of three separate experiments; (C) viability, detected by MTT assay (absorbance of control cells 0.63 ± 0.05 was assumed as 100%), and NO production, detected by Griess reagent (absorbance of control cells 0.29 ± 0.05 was assumed as 100%.) after a 24 h LPS exposure. Data represent means ± SD ($n = 3$). *$p < 0.05$.

NO levels found in the presence of cyclo(His-Pro). These data suggest that cyclo(His-Pro), by reducing NF-κB activation inhibits iNOS expression and, consequently NO production.

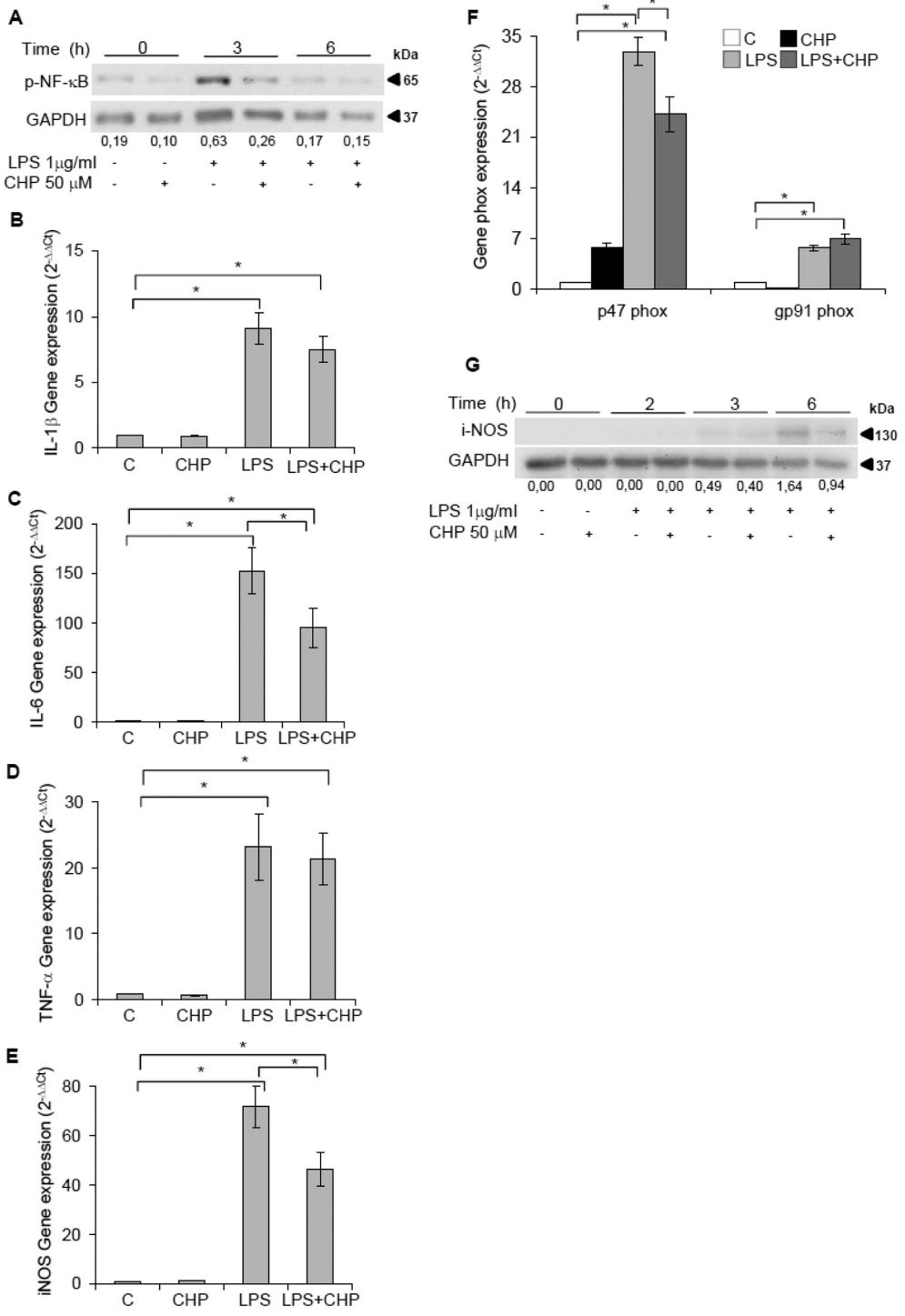

Fig. 3. Cyclo(His-Pro) reduces NO production by inhibiting NF-κB. hSOD1(G93A) microglial cells were pretreated for 24 h with 50 μM CHP and then treated with 1 μg/ml LPS. (A) Time course of *p*-NF-κB (p65). At each indicated time, cells were collected and total extract analysed by Western blotting. GAPDH was used as loading control. Numbers below the images represent the ratio between *p*-NF-κB and GAPDH band intensity The images are representative of one out of three separate experiments; qRT-PCR of IL-1β (B), IL-6 (C), TNF-α (D), iNOS (E), and p47 and gp91 phox (F) after a 6 h LPS exposure. Gene expression values were normalized to Gapdh and presented as $2^{-\Delta\Delta Ct}$. Relative mRNA gene abundance in untreated cells was assumed to be 1 (control). Data represent mean ± SD ($n = 3$). *$p < 0.05$; (G) time course of iNOS. At each indicated time, cells were collected and total extract analysed by Western Blotting. GAPDH was used as loading control. Numbers below the images represent the ratio between iNOS and GAPDH band intensity The images are representative of one out of three separate experiments.

3.4. Cyclo(His-Pro) reduces ROS levels without affecting Nrf2 in hSOD1(G93A) microglial cells

Although cyclo(His-Pro) did not reduce NOX2 catalytic subunit gene expression (Fig. 3F), we observed that it was capable of inducing a decrease in ROS levels. Therefore, we first examined whether cyclo(His-Pro) could counteract ROS generation by increasing Nrf2-driven antioxidant gene expression. We found that in hSOD1(G93A) microglial cells, LPS induces an increase in Nrf2 nuclear translocation (Fig. 4A) accompanied by an increase in antioxidant gene expression (Fig. 4B). On the contrary, the 24 h cyclo(His-Pro) pre-treatment does not increase either Nrf2 nuclear translocation (Fig. 4A) or the expression of antioxidant genes (Fig. 4B). These results indicate that the reduction in ROS levels are not dependent on increased antioxidant defences driven by cyclo(His-Pro).

3.5. Cyclo(His-Pro) increases soluble SOD1 activity

It is to note that hSOD1(G93A) mutation induces the aggregation of the enzyme that acquire a toxic gain of function supporting the pathogenesis of ALS (Strong et al., 2005). It has been reported that SOD1 mutations can cause protein misfolding that, in turn, lead to the inhibition of the ubiquitin-proteasome system, and enhanced pro-inflammatory ROS production (Franco et al., 2013). To test whether cyclo

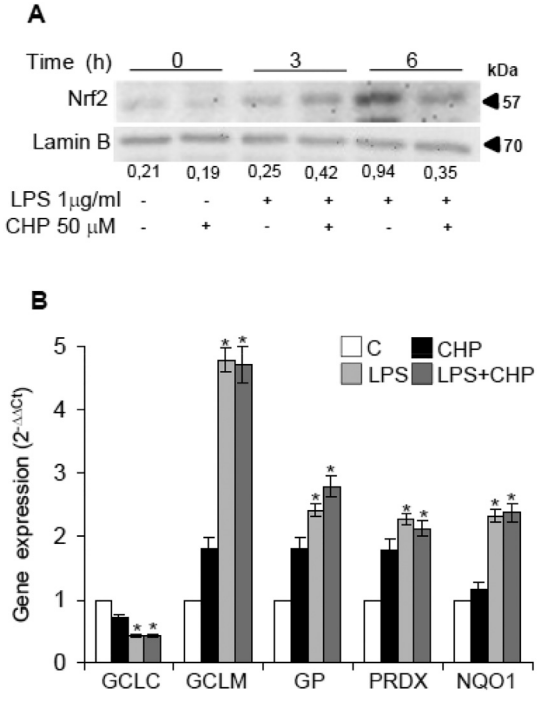

Fig. 4. Cyclo(His-Pro) reduces ROS levels without affecting Nrf2. hSOD1(G93A) microglial cells were pretreated for 24 h with 50 μM CHP and then exposed to 1 μg/ml LPS. (A) Time course of Nrf2. At each indicated time, cells were collected and nuclear extract analysed by Western blotting. Lamin B was used as loading control. Numbers below the images represent the ratio between Nrf2 and lamin B band intensity The images are representative of one out of three separate experiments; (B) qRT-PCR of the indicated genes after a 3 h LPS exposure. Gene expression values were normalized to Gapdh and presented as $2^{-\Delta\Delta Ct}$. Relative mRNA gene abundance in untreated cells was assumed as 1 (control). Data represent mean ± SD ($n = 3$). *$p < 0.05$ vs. control cells.

(His-Pro) could reduce protein aggregation in hSOD1(G93A) microglial cells, we measured Thioflavin T fluorescence after a 4-days cyclo(His-Pro) exposure and found it slightly but significantly reduced (Fig. 5A), suggesting that cyclo(His-Pro) can reduce the amount of protein aggregates. The clearance of misfolded aggregates can rely on: an increase in ubiquitin-proteasome system function, an increase in the autophagic flux, and an increase in Hsps expression. We first analysed the involvement of ubiquitin-proteasome system on cyclo(His-Pro) induced effects. We found that cyclo(His-Pro) does not affect the poly-ubiquitination process as evidenced by unchanged levels of poly-ubiquitinated proteins in any tested conditions (Fig. 5B). Moreover, we found no differences in the autophagy marker LC3 upon cyclo(His-Pro) treatment (Fig. 5C). We then tested the possible effects of cyclo(His-Pro) on gene expression of molecular chaperones Hsp27, Hsp70 and Hsp72 and found that the expression of Hsp27 and Hsp70 is significantly increased by cyclo(His-Pro) pre-treatment compared to a 6 h LPS exposure (Fig. 5D). These data suggest that cyclo(His-Pro) can reduce protein aggregation by increasing the cellular protein folding ability.

To understand whether the effects of cyclo(His-Pro) underlie an increase in soluble SOD1 activity, we measured specific enzyme activity in the soluble and insoluble fractions of cell lysates (Fig. 5E) and found that pre-treatment with cyclo(His-Pro) increased SOD1 activity in the soluble fraction, while reducing enzyme activity in the insoluble fraction. This data suggest that the reduced amount of ROS detected in the presence of cyclo(His-Pro) might depend on the increased levels of catalytically-active soluble SOD1.

4. Discussion

In this paper we showed that cyclo(His-Pro), by lowering mutant SOD1 aggregation, prevents LPS-induced inflammasome activation in an ALS microglial cell model.

Abnormal protein aggregation in both neurons and glia is a hallmark of several neurodegenerative diseases, including amyotrophic lateral sclerosis (ALS). For this reason, neurodegenerative diseases can be regarded as a protein misfolding disorders (Hekmatimoghaddam et al., 2017; Forsberg et al., 2011). The incorrect folding of mutant SOD1 induces a toxic gain of function that has been explained either with an aberrant catalysis that causes an increase in ROS production or with the toxic effects of aggregates themselves (Franco et al., 2013; Strong et al., 2005). The aberrant catalysis hypothesis states that the mutated enzyme can have a reduced ability to catalyze the disproportionation of superoxide or can catalyze the reverse reaction converting hydrogen peroxide to superoxide anion which, combining with NO, generates peroxynitrite. Moreover, mutant SOD1 can catalyze tyrosine nitration (Yim et al., 1990; Este'vez et al., 1999; Franco et al., 2013). We have previously shown that peroxynitrite production, through nitration of tyrosine residues, causes the activation of NLRP3 inflammasome, with the consequent cleavage of caspase 1 and maturation and secretion of IL-1β in microglial cells harbouring the G93A mutation in the SOD1 protein (Bellezza et al., 2018). In this report we showed that the diketopiperazine cyclo(His-Pro), by reducing the levels of nitrated proteins, inhibits LPS-induced inflammasome activation in the microglial model of ALS.

The activation of inflammasome relies on peroxynitrite production which is due to the increase in iNOS and NOX2 activity (Bellezza et al., 2018). Both iNOS and NOX2 genes are controlled by the transcription factor NF-κB, whose activation depends, among other, on the binding of LPS to Toll-like receptor 4 (TLR4) (Doyle and O'Neill, 2006). Cyclo(His-Pro) exerts its anti-inflammatory actions by inhibiting NF-κB activation in several cellular models of neuroinflammation (Bellezza et al., 2014a, 2014b; Minelli et al., 2012). In microglial cells harbouring the G93A substitution in SOD1 gene, as expected, pre-treatment with cyclo(His-Pro) reduces the phosphorylation of p65 subunit of NF-κB and the expression of several NF-κB regulated genes. It is to note that cyclo(His-Pro)-induced inhibition of NF-κB well correlates with a reduced iNOS gene and protein expression and enzyme activity, as evidenced by the reduction in NO levels. On the other hand, cyclo(His-Pro) does not reduce the expression of gp91phox catalytic subunit of NOX2, although reducing ROS levels. It has been reported that cyclo(His-Pro) can activate Nrf2 (Minelli et al., 2009a, 2009b), the major transcription factor for cellular antioxidant defences (Silva-Islas and Maldonado, 2018), and through the induction of hemeoxygenase 1 expression can downregulate NF-κB (Minelli et al., 2012; Bellezza et al., 2012; Bellezza et al., 2014a, 2014b). We therefore speculated whether the antioxidant properties of cyclo(His-Pro) could be responsible for the observed effect on ROS levels. Although the cyclic dipeptide activates Nrf2 in the ALS microglial cells stimulated with a pro-oxidant (Grottelli et al., 2015), it does not induce Nrf2 activation and the transcription of target genes in the same cells stimulated with LPS. Therefore, other cellular mechanisms should be responsible for the cyclo(His-Pro)-induced decrease in ROS levels.

The aberrant catalysis determined by an incorrect folding of SOD1can be avoided either by increasing the clearance of aggregates through autophagy or ubiquitin-proteasome system, or by ameliorating the folding process through an increase in molecular chaperone expression (Grottelli et al., 2018). In our experimental conditions, we observed that cyclo(His-Pro) does not modify the amount of either LC3B or ubiquitinated proteins, thus suggesting that the increase in aggregates removal cannot be regarded as the cause of the observed reduction in Thioflavin T stained protein aggregates. On the other hand, a plausible explanation for the decreased amount of protein aggregates could rely on the cyclo(His-Pro) –induced expression of the molecular

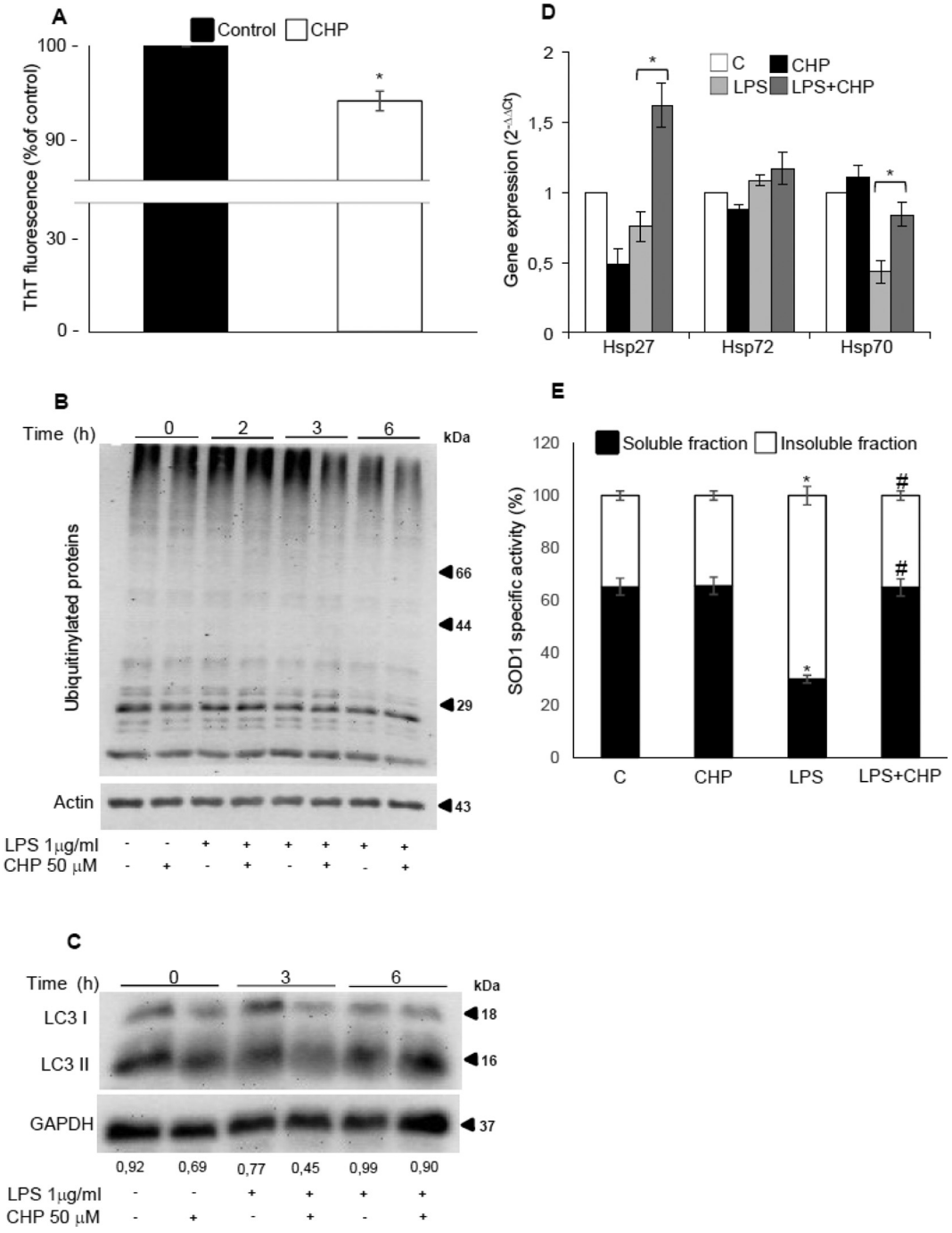

Fig. 5. Cyclo(His-Pro) increases soluble SOD1 activity. hSOD1(G93A) microglial cells were treated for four days with 50 μM CHP and used for determination of Thioflavin T fluorescence. Data represent means ± SD ($n = 3$) *$p < 0.05$ vs. control cells. SOD1(G93A) microglial cells were pretreated for 24 h with 50 μM CHP and then exposed to 1 μg/ml LPS. Time course of poly-ubiquitination proteins (B) and LC3(C). At each indicated time, cells were collected and total extract analysed by Western blotting. Actin and GAPDH were used as loading control. Numbers below the images represent the ratio between LC3 II and GAPDH band intensity. The images are representative of one out of three separate experiments; (D) qRT-PCR of the indicated genes after 6 h LPS exposure. Gene expression values were normalized to Gapdh and presented as $2^{-\Delta\Delta Ct}$. Relative mRNA gene abundance in untreated cells was assumed as 1 (control). Data represent mean ± SD ($n = 3$). *$p < 0.05$ vs. LPS treated cells; (E) determination of SOD1 specific activity after 24 h LPS treatment. Data were presented as percentage of protein in the soluble and insoluble fractions of the lysate. Data represent mean ± SD ($n = 3$). *$p < 0.05$ vs. untreated cells. $^{\#}p < 0.05$ vs. LPS treated cells.

chaperones Hsp27 and Hsp70. This finding is in agreement with our previous data showing that the cyclic dipeptide increases Hsp27 and α-B-Crystallin in serum starved PC12 cells (Minelli et al., 2006). Therefore, while Hsp27 suppresses SOD1 aggregation in vitro (Yerbury et al., 2013), the treatment with of cyclo(His-Pro) increases soluble SOD1 enzyme activity. Due to the fact that SOD1 converts superoxide anion, produced by NOX2, in the less reactive hydrogen peroxide, the increased activity of SOD1 in the presence of cyclo(His-Pro) might explain the reduction in ROS levels and the consequent inhibition of inflammasome. The use of ebselen, an antioxidant compound that efficiently directs correct SOD1 folding to rescue the toxic characteristics of mutant SOD1 (Capper et al., 2018) corroborates our hypothesis.

5. Conclusion

Our results indicate that cyclo(His-Pro) inhibits inducible nitric oxide synthase and, by inducing Hsps expression, promotesSOD1 correct folding, thus reducing inflammasome activation in an ALS microglial cell model. It is worth mentioning that cyclo(His-Pro) is well tolerated in humans and has been already formulated for oral administration to treat type 1 diabetes (Grottelli et al., 2016; Uyemura et al., 2010; Choi et al., 2017). All this considered, cyclo(His-Pro) can be view as a good candidate for the treatment of ALS.

Supplementary data to this article can be found online at https://doi.org/10.1016/j.mcn.2018.11.002.

Acknowledgements

We thank Dr G. Pietrini (Università di Milano) for providing immortalized hSOD1(G93A) microglial cells.

The work was supported by the Basic Research Funding 2017 of the Department of Experimental Medicine to IB (#FFRB17IB).

References

Bellezza, I., Tucci, A., Galli, F., Grottelli, S., Mierla, A.L., Pilolli, F., Minelli, A., 2012. Inhibition of NF-κB nuclear translocation via HO-1 activation underlies α-tocopheryl succinate toxicity. J. Nutr. Biochem. 23, 1583–1591.

Bellezza, I., Peirce, M.J., Minelli, A., 2014a. Cyclic dipeptides: from bugs to brain. Trends Mol. Med. 20, 551–558.

Bellezza, I., Grottelli, S., Mierla, A.L., Cacciatore, I., Fornasari, E., Roscini, L., Cardinali, G., Minelli, A., 2014b. Neuroinflammation and endoplasmic reticulum stress are coregulated by cyclo(His-Pro) to prevent LPS neurotoxicity. Int. J. Biochem. Cell Biol. 51, 159–169.

Bellezza, I., Grottelli, S., Costanzi, E., Scarpelli, P., Pigna, E., Morozzi, G., Mezzasoma, L., Peirce, M.J., Moresi, V., Adamo, S., Minelli, A., 2018. Peroxynitrite activates the NLRP3 inflammasome cascade in SOD1(G93A) mouse model of amyotrophic lateral sclerosis. Mol. Neurobiol. 55, 2350–2361.

Capper, M.J., Wright, G.S.A., Barbieri, L., Luchinat, E., Mercatelli, E., McAlary, L., Yerbury, J.J., O'Neill, P.M., Antonyuk, S.V., Banci, L., Hasnain, S.S., 2018. The cysteine-reactive small molecule ebselen facilitates effective SOD1 maturation. Nat. Commun. 9, 1693.

Choi, B.Y., Kim, I.Y., Kim, J.H., Lee, B.E., Lee, S.H., Kho, A.R., Sohn, M., Suh, S.W., 2017. Administration of zinc plus cyclo-(His-Pro) increases hippocampal neurogenesis in rats during the early phase of streptozotocin-induced diabetes. Int. J. Mol. Sci. 18 (pii: E73).

Doyle, S.L., O'Neill, L.A., 2006. Toll-like receptors: from the discovery of NFkappaB to new insights into transcriptional regulations in innate immunity. Biochem. Pharmacol. 72, 1102–1113.

Este'vez, A.G., Crow, J.P., Sampson, J.B., et al., 1999. Induction of nitric oxide dependent apoptosis in motor neurons by zinc-deficient superoxide dismutase. Science 286, 2498–2500.

Eruslanov, E., Kusmartsev, S., 2010. Identification of ROS using oxidized DCFDA and flow-cytometry. Methods Mol. Biol. 594, 57–72.

Ferrer-Sueta, G., Radi, R., 2009. Chemical biology of peroxynitrite: kinetics, diffusion, and radicals. ACS Chem. Biol. 4, 161–177.

Forsberg, K., Andersen, P.M., Marklund, S.L., Brännström, T., 2011. Glial nuclear aggregates of superoxide dismutase-1 are regularly present in patients with amyotrophic lateral sclerosis. Acta Neuropathol. 121, 623–634.

Franco, M.C., Dennys, C.N., Rossi, F.H., Estévez, A.G., 2013. Superoxide dismutase and oxidative stress in amyotrophic lateral sclerosis. In: Chapter 5 in Current Advances in Amyotrophic Lateral Sclerosis. InThech Open.

Grottelli, S., Bellezza, I., Morozzi, G., Peirce, M.J., Marchetti, C., Cacciatore, I., Costanzi, E., Minelli, A., 2015. Cyclo (His-Pro) protects SOD1G93A microglial cells from paraquat–induced toxicity. J. Clin. Cell Immunol. 6, 287.

Grottelli, S., Ferrari, I., Pietrini, G., Peirce, M.J., Minelli, A., Bellezza, I., 2016. The role of cyclo(His-Pro) in neurodegeneration. Int. J. Mol. Sci. 17 (8) (pii: E1332).

Grottelli, S., Costanzi, E., Peirce, M.J., Minelli, A., Cellini, B., Bellezza, I., 2018. Potential influence of cyclo(His-Pro) on proteostasis: impact on neurodegenerative diseases. Curr. Protein Pept. Sci. 19, 805–812.

Hekmatimoghaddam, S., Zare-Khormizi, M.R., Pourrajab, F., 2017. Underlying mechanisms and chemical/biochemical therapeutic approaches to ameliorate protein misfolding neurodegenerative diseases. Biofactors 43, 737–759.

Kiernan, M.C., Vucic, S., Cheah, B.C., Turner, M.R., Eisen, A., Hardiman, O., Burrell, J.R., Zoing, M.C., 2011. Amyotrophic lateral sclerosis. Lancet 377, 942–955.

Kukla, M.J., Breslin, H.J., Bowden, C.R., 1985. Synthesis, characterization, and anorectic testing of the four stereoisomers of cyclo(histidylproline). J. Med. Chem. 28, 1745–1747.

Li, M., Ona, V.O., Guégan, C., Chen, M., Jackson-Lewis, V., Andrews, L.J., Olszewski, A.J., Stieg, P.E., Lee, J.P., Przedborski, S., Friedlander, R.M., 2000. Functional role of caspase-1 and caspase-3 in an ALS transgenic mouse model. Science 288, 335–339.

Meissner, F., Molawi, K., Zychlinsky, A., 2010. Mutant superoxide dismutase 1-induced IL-1beta accelerates ALS pathogenesis. Proc. Natl. Acad. Sci. U. S. A. 107, 13046–13050.

Minelli, A., Bellezza, I., Grottelli, S., Pinnen, F., Brunetti, L., Vacca, M., 2006. Phosphoproteomic analysis of the effect of cyclo-[His-Pro] dipeptide on PC12 cells. Peptides 27, 105–113.

Minelli, A., Conte, C., Grottelli, S., Bellezza, I., Emiliani, C., Bolaños, J.P., 2009a. Cyclo (His-Pro) up-regulates heme oxygenase 1 via activation of Nrf2-ARE signalling. J. Neurochem. 111, 956–966.

Minelli, A., Conte, C., Grottelli, S., Bellezza, I., Cacciatore, I., Bolaños, J.P., 2009b. Cyclo (His-Pro) promotes cytoprotection by activating Nrf2-mediated up-regulation of antioxidant defence. J. Cell. Mol. Med. 13, 1149–1161.

Minelli, A., Grottelli, S., Mierla, A., Pinnen, F., Cacciatore, I., Bellezza, I., 2012. Cyclo(His-Pro) exerts anti-inflammatory effects by modulating NF-κB and Nrf2 signalling. Int. J. Biochem. Cell Biol. 44, 525–535.

Righi, M., Pierani, A., Boglia, A., De Libero, G., Mori, L., Marini, V., Ricciardi-Castagnoli, P., 1989. Generation of new oncogenic murine retroviruses by cotransfection of cloned AKR and MH2 proviruses. Oncogene 4, 223–230.

Rosen, D.R., Siddique, T., Patterson, D., Figlewicz, D.A., Sapp, P., Hentati, A., Donaldson, D., Goto, J., O'Regan, J.P., Deng, H.X., 1993. Mutations in Cu/Zn superoxide dismutase gene are associated with familial amyotrophic lateral sclerosis. Nature 362, 59–62.

Ruegsegger, C., Saxena, S., 2016. Proteostasis impairment in ALS. Brain Res. 1648 (Pt B), 571–579.

Shi, F., Kouadir, M., Yang, Y., 2015. NALP3 inflammasome activation in protein misfolding diseases. Life Sci. 135, 9–14.

Silva-Islas, C.A., Maldonado, P.D., 2018. Canonical and non-canonical mechanisms of Nrf2 activation. Pharmacol. Res. 134, 92–99.

Singhal, G., Jaehne, E.J., Corrigan, F., Toben, C., Baune, B.T., 2014. Inflammasomes in neuroinflammation and changes in brain function: a focused review. Front. Neurosci. 8, 315.

Strong, M.J., Kesavapany, S., Pant, H.C., 2005. The pathobiology of amyotrophic lateral sclerosis: a proteinopathy? J. Neuropathol. Exp. Neurol. 64, 649–664.

Uyemura, K., Dhanani, S., Yamaguchi, D.T., Song, M.K., 2010. Metabolism and toxicity of high doses of cyclo(His-Pro) plus zinc in healthy human subjects. J. Drug Metab. Toxicol. 1, 105.

Volpe, C.M., Nogueira-Machado, J.A., 2015. Is innate immunity and inflammasomes involved in pathogenesis of amyotrophic lateral sclerosis (ALS)? Recent Patents Endocr. Metab. Immune Drug Discov. 9, 40–45.

Yerbury, J.J., Gower, D., Vanags, L., Roberts, K., Lee, J.A., Ecroyd, H., 2013. The small heat shock proteins αB-crystallin and Hsp27 suppress SOD1 aggregation in vitro. Cell Stress Chaperones 18, 251–257.

Yim, M.B., Chock, P.B., Stadtman, E.R., 1990. Copper, zinc superoxide dismutase catalyzes hydroxyl radical production from hydrogen peroxide. Proc. Natl. Acad. Sci. U. S. A. 87, 5006–5010.